High-Nuclearity Metal-Cyanide Clusters: Assembly of a $Cr_8Ni_6(CN)_{24}$ Cage with a Face-Centered Cubic Geometry

Polly A. Berseth, Jennifer J. Sokol, Matthew P. Shores, Julie L. Heinrich, and Jeffrey R. Long*

Contribution from the Department of Chemistry, University of California, Berkeley, California 94720-1460

Received June 5, 2000

Abstract: The synthesis of high-nuclearity metal-cyanide clusters presents a possible means of controlling magnetic properties in the design of new single-molecule magnets. Previous work employed tridentate blocking ligands in directing the assembly of a cubic $[(tacn)_8Co_8(CN)_{12}]^{12+}$ (tacn = 1,4,7-triazacyclononane) cluster; an improved crystal structure now confirms the lack of a guest water molecule inside the cluster cage. The ability to generate larger clusters by using a blocking ligand on only one of the mononuclear reaction components is demonstrated with the synthesis of a fourteen-metal $[(Me_3tacn)_8Cr_8Ni_6(CN)_{24}]^{12+}$ cluster. The geometry of this cluster consists of a cube of eight Me_3tacn-ligated Cr^{III} ions connected via bridging cyanide ligands to six square-planar Ni^{II} ions situated just above the center of each cube face. Surprisingly, no guest species are evident within the 284 $Å^3$ cavity defined by the rigid metal-cyanide cage. Assembly of the cluster in boiling aqueous solution involves a linkage isomerization wherein the carbon end of each cyanide ligand reorients from binding a Cr^{III} center in the reactant to binding the softer Ni^{II} center in the product. Consequently, the Ni^{II} ions become diamagnetic, resulting in magnetic behavior at high temperatures that is consistent with eight isolated Cr^{III} ($S = 3/2$) ions per cluster. However, below 30 K, a drop in the $\chi^M T$ is attributed to weak antiferromagnetic coupling between Cr^{III} ions through the LUMO orbitals of the $[Ni(CN)_4]^{2-}$-like units centering each cluster face. Carrying out the assembly reaction in methanol at −40 °C forestalls the linkage isomerization, yielding a high-spin green form of the cluster. Reaction of $[(Me_3tacn)_8Cr_8Ni_6(CN)_{24}]^{12+}$ with $[Ni(CN)_4]^{2-}$ affords an aggregate species with a tetracyanonickelate ion capping each face of the cluster through a mean Ni⋯Ni contact of 3.00(1) Å, an interaction that destroys the long-range antiferromagnetic coupling between Cr^{III} ions. Efforts to construct a larger cluster with an edge-bridged cubic geometry produced a linear $[(Me_3tacn)_2(cyclam)NiCr_2(CN)_6]^{2+}$ (cyclam = 1,4,8,11-tetraazacyclotetradecane) fragment exhibiting an $S = 4$ ground state. The weak ferromagnetic coupling ($J = 10.9$ cm^{-1}) within this cluster leads to a more rapid decrease in the magnetization with increasing temperature at higher magnetic fields as a result of the Zeeman splitting and population of low-lying excited states.

Introduction

It was recently shown that certain high-spin clusters, dubbed single-molecule magnets, are capable of sustaining a remanent magnetization at low temperature upon removal from a polarizing field.[1] These clusters possess an axial magnetic anisotropy ($D < 0$) stemming from zero-field splitting in the ground state that gives rise to an energy barrier for magnetic moment reversal. Thus, magnetic hysteresis results from an extremely long magnetic relaxation time, rather than from the motion of magnetic domain walls (as in a bulk ferromagnet). For a single-molecule magnet with integral spin S, this energy barrier is given by $S^2|D|$. The largest barrier yet observed is approximately 50 cm^{-1}, occurring in the $S = 10$ cluster $[Mn_{12}O_{12}(CH_3CO_2)_{16}(H_2O)_4]$, which exhibits a magnetic relaxation half-life of two months at 2 K.[1b] For potential data storage applications, in which each cluster ideally would represent a single bit of information (either spin up or spin down along the preferred axis), an increase in the barrier height is of obvious benefit to the temperature and duration of storage.[2] However, all of the single-molecule magnets reported to date originate from metal-oxo cluster systems, wherein the enormous structural variability curtails synthetic control over geometry and magnetic properties. Developing alternative cluster systems with better prospects for controlling S and D, therefore, presents a worthwhile challenge.

* To whom correspondence should be addressed.

(1) (a) Sessoli, R.; Tsai, H.-L.; Schake, A. R.; Wang, S.; Vincent, J. B.; Folting, K.; Gatteschi, D.; Christou, G.; Hendrickson, D. N. *J. Am. Chem. Soc.* **1993**, *115*, 1804. (b) Sessoli, R.; Gatteschi, D.; Caneschi, A.; Novak, M. A. *Nature* **1993**, *365*, 141. (c) Eppley, H. J.; Tsai, H.-L.; de Vries, N.; Folting, K.; Christou, G.; Hendrickson, D. N. *J. Am. Chem. Soc.* **1995**, *117*, 301. (d) Aubin, S. M. J.; Wemple, M. W.; Adams, D. M.; Tsai, H.-L.; Christou, G.; Hendrickson, D. N. *J. Am. Chem. Soc.* **1996**, *118*, 7746. (e) Barra, A.-L.; Debrunner, P.; Gatteschi, D.; Schultz, C. E.; Sessoli, R. *Europhys. Lett.* **1996**, 35, 133. (f) Castro, S. L.; Sun, Z.; Grant, C. M.; Bolinger, J. C.; Hendrickson, D. N.; Christou, G. *J. Am. Chem. Soc.* **1998**, *120*, 2365. (g) Brechin, E. K.; Yoo, J.; Nakano, M.; Huffman, J. C.; Hendrickson, D. N.; Christou, G. *Chem. Commun.* **1999**, 783. (h) Barra, A. L.; Caneschi, A.; Cornia, A.; Fabrizi de Biani, F.; Gatteschi, D.; Sangregorio, C.; Sessoli, R.; Sorace, L. *J. Am. Chem. Soc.* **1999**, *121*, 5302. (i) Aubin, S. M. J.; Sun, Z.; Pardi, L.; Krzystek, J.; Folting, K.; Brunel, L.-C.; Rheingold, A. L.; Christou, G.; Hendrickson, D. N. *Inorg. Chem.* **1999**, *38*, 5329.

(2) Further motivation for studying these clusters derives from a desire to understand physical phenomena, such as quantum tunneling of magnetization, that are particular to the regime between molecular and bulk magnetism. See: (a) Friedman, J. R.; Sarachik, M. P.; Tejada, J.; Ziolo, R. *Phys. Rev. Lett.* **1996**, *76*, 3830. (b) Thomas, L.; Lionti, F.; Ballou, R.; Gatteschi, D.; Sessoli, R.; Barbara, B. *Nature* **1996**, *383*, 145. (c) Luis, F.; Bartolomé, J.; Fernández, J. F.; Tejada, J.; Hernández, J. M.; Zhang, X. X. *Phys. Rev. B* **1997**, *55*, 11448. (d) Aubin, S. M. J.; Dilley, N. R.; Pardi, L.; Krzystek, J.; Wemple, M. W.; Brunel, L.-C.; Maple, M. B.; Christou, G.; Hendrickson, D. N. *J. Am. Chem. Soc.* **1998**, *120*, 4991 and references therein.

Toward this end, we have begun to explore transition metal-cyanide cluster chemistry.[3,4] While an oxide ion can connect as many as six different metal centers through a range of possible M−O−M angles, cyanide bridges are generally restricted to a linear arrangement spanning just two metal centers. Consequently, in designing cyano-bridged materials, it is easier to predict both the structural outcome of an assembly reaction and the nature of the magnetic exchange interaction between pairs of metal centers. Such factors have previously been recognized and exploited with the preparation of metal-cyanide solids exhibiting bulk magnetic ordering. Formed in aqueous assembly reactions between octahedral $[M(H_2O)_6]^{x+}$ and $[M'(CN)_6]^{y-}$ complexes, these compounds adopt structures of the type observed for Prussian blue[5] which consist of a simple cubic three-dimensional framework built up from linear M'−CN−M linkages.[6] By varying the transition metals M and M' in the reactants, the nature (ferromagnetic or antiferromagnetic) and strength of the exchange coupling can be adjusted, permitting synthesis of materials with magnetic ordering temperatures as high as 373 K.[7] Wielded in the design of molecular clusters instead of extended solids, a similar measure of control could greatly facilitate the synthesis of new single-molecule magnets.

As an initial test of our ability to direct the structure of metal-cyanide clusters, we set out to construct molecules consisting of just one of the fundamental cubic cage units comprising the Prussian blue framework. The approach employed parallels the solid assembly process but uses the tridentate ligand 1,4,7-triazacyclononane (tacn) to block a single face in the octahedral coordination sphere of each of the transition metal reactants, thereby preventing growth of an extended solid framework.

$$4[(tacn)M(H_2O)_3]^{x+} + 4[(tacn)M'(CN)_3]^{y-} \rightarrow$$
$$[(tacn)_8M_4M'_4(CN)_{12}]^{4(x-y)+} \quad (1)$$
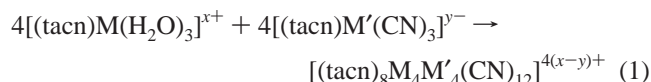
This strategy yielded two such molecular Prussian blue analogues: $[(tacn)_8Cr_4Co_4(CN)_{12}]^{12+}$ and $[(tacn)_8Co_8(CN)_{12}]^{12+}$.[3] The structure of the latter species is shown in Figure 1, and, indeed, consists of the anticipated cube of eight Co^{III} ions with each edge spanned by a linear cyanide bridge and each corner capped by a tacn ligand. Analogous clusters containing cyclopentadienyl and carbonyl ligands have also been reported recently.[8] By synthesizing the appropriate paramagnetic precursors, it should be possible to use reaction 1 to construct cubic
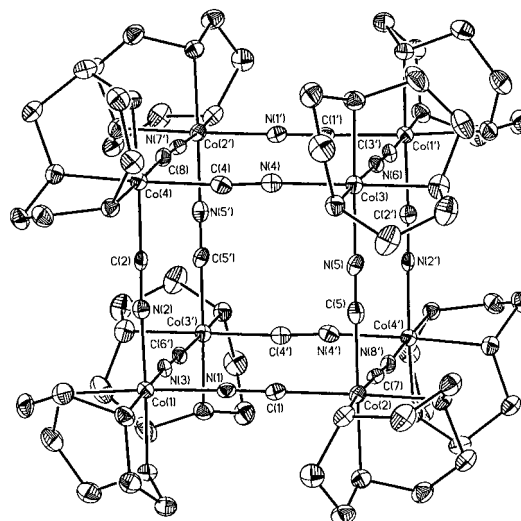

Figure 1. Structure of the cubic $[(tacn)_8Co_8(CN)_{12}]^{12+}$ cluster in compound **1**, showing 50% probability ellipsoids and the core-atom labeling scheme; H atoms are omitted for clarity. The cluster, which resides on an inversion center in the crystal structure, was modeled as being disordered between two core orientations: the one depicted and that obtained upon applying the inversion operation. Selected mean interatomic distances (Å) and angles (deg) (X is a cyanide C or N atom): Co−X, 1.898(6); Co−N, 1.947(7); X−X, 1.151(3); Co···Co, 4.94(1); X−Co−X, 90(1); Co−X−X, 177(2); N−Co−X, 92(1); N−Co−N, 86.0(2).

clusters possessing ground-state configurations with total spin ranging over the even integral values from $S = 0$ to $S = 10$.[9] However, the maximum spin attainable with this geometry ($S = 10$ might be realized with, for example, M = Ni^{II} and M' = Cr^{III}) is no greater than the spin of the aforementioned Mn$_{12}$ single-molecule magnet. To generate the exceptionally large spin states ultimately desired, it is necessary to develop methods for producing higher-nuclearity clusters in which even more metal centers can be magnetically coupled.

A simple idea for achieving larger clusters is to carry out assembly reactions with a blocking tacn ligand on only one of the components in reaction 1, thus permitting growth to propagate further before the cluster closes up into a cage. Herein, we report an implementation of this approach with the synthesis of $[(Me_3tacn)_8Cr_8Ni_6(CN)_{24}]^{12+}$ (Me$_3$tacn = *N,N',N''*-trimethyl-1,4,7-triazacyclononane), a fourteen-metal cluster with an unprecedented face-centered cubic geometry.

Experimental Section

Preparation of Compounds. Crude Me$_3$tacn obtained from Unilever was purified by vacuum distillation (36 °C, ca. 80 mTorr) prior to use. The compounds $[(tacn)_8Co_8(CN)_{12}](C_7H_7SO_3)_{12} \cdot 24H_2O$ (**1**) and Ni-(cyclam)(ClO$_4$)$_2$ were synthesized as described previously.[3,10] The reactant $[(Me_3tacn)Cr(CF_3SO_3)_3]$ was prepared in a manner analogous to that reported for $[(tacn)Cr(CF_3SO_3)_3]$.[11] Water was distilled and deionized with a Milli-Q filtering system. All other reagents were obtained from commercial vendors and used without further purification.

(3) Heinrich, J. L.; Berseth, P. A.; Long, J. R. *Chem. Commun.* **1998**, 1231.

(4) Others have also noted the facility of regulating spin in metal-cyanide clusters: (a) Mallah, T.; Auberger, C.; Verdaguer, M.; Veillet, P. *J. Chem. Soc., Chem. Commun.* **1995**, 61. (b) Scuiller, A.; Mallah, T.; Verdaguer, M.; Nivorozhkin, A.; Tholence, J.-L.; Veillet, P. *New J. Chem.* **1996**, *20*, 1.

(5) Buser, H. J.; Schwarzenbach, D.; Petter, W.; Ludi, A. *Inorg. Chem.* **1977**, *16*, 2704.

(6) (a) Shriver, D. F.; Shriver, S. A.; Anderson, S. E. *Inorg. Chem.* **1965**, *4*, 725. (b) Dunbar, K. R.; Heintz, R. A. *Prog. Inorg. Chem.* **1997**, *45*, 283 and references therein.

(7) (a) Gadet, V.; Mallah, T.; Castro, I.; Verdaguer, M. *J. Am. Chem. Soc.* **1992**, *114*, 9213. (b) Mallah, T.; Thiébaut, S.; Verdaguer, M.; Veillet, P. *Science* **1993**, *262*, 1554. (c) Entley, W. R.; Girolami, G. S. *Science* **1995**, *268*, 397. (d) Ferlay, S.; Mallah, T.; Ouahès, R.; Veillet, P.; Verdaguer, M. *Nature* **1995**, *378*, 701. (e) Entley, W. R.; Treadway, C. R.; Girolami, G. S. *Mol. Cryst. Liq. Cryst.* **1995**, *273*, 153. (f) Dujardin, E.; Ferlay, S.; Phan, X.; Desplanches, C.; Cartier dit Moulin, C.; Sainctavit, P.; Baudelet, F.; Dartyge, E.; Veillet, P.; Verdaguer, M. *J. Am. Chem. Soc.* **1998**, *120*, 11347. (g) Holmes, S. M.; Girolami, G. S. *J. Am. Chem. Soc.* **1999**, *121*, 5593. (h) Hatlevik, Ø.; Buschmann, W. E.; Zhang, J.; Manson, J. L.; Miller, J. S. *Adv. Mater.* **1999**, *11*, 914.

(8) (a) Klausmeyer, K. K.; Rauchfuss, T. B.; Wilson, S. R. *Angew. Chem., Int. Ed. Engl.* **1998**, *37*, 1694. (b) Klausmeyer, K. K.; Wilson, S. R.; Rauchfuss, T. B. *J. Am. Chem. Soc.* **1999**, *121*, 2705.

(9) Predicted spin states are based on the coupling rules previously established for Prussian blue-type solids.[7] For octahedral metal centers, unpaired electrons in adjacent metal orbitals that belong to the same representation ($t_{2g} + t_{2g}$ or $e_g + e_g$) couple antiferromagnetically through cyanide, while those in orthogonal orbitals ($t_{2g} + e_g$) couple ferromagnetically. Antiferromagnetic interactions through cyanide π^* orbitals are typically much stronger than the ferromagnetic interactions and will dominate in a competitive situation.

(10) Bosnich, B.; Tobe, M. L.; Webb, G. A. *Inorg. Chem.* **1965**, *4*, 1109.

(11) Ryu, C. K.; Lessard, R. B.; Lynch, D.; Endicott, J. F. *J. Phys. Chem.* **1989**, *93*, 1752.

Table 1. Crystallographic Data[a] for $[(tacn)_8Co_8(CN)_{12}](C_7H_7SO_3)_{12}\cdot24H_2O$ (**1**), $[(Me_3tacn)Cr(CN)_3]\cdot H_2O$ (**2**·H₂O), $[(Me_3tacn)_8Cr_8Ni_6(CN)_{24}](NO_3)_{12}\cdot54H_2O$ (**3**·37H₂O), $[(Me_3tacn)_8Cr_8Ni_6(CN)_{24}]Br_{12}\cdot45H_2O$ (**4**·17H₂O), $[(Me_3tacn)_8Cr_8Ni_6(CN)_{24}][Ni(CN)_4]_6\cdot47H_2O$ (**5**·28H₂O), and $[(Me_3tacn)_2(cyclam)NiCr_2(CN)_6](ClO_4)_2\cdot2H_2O$ (**6**)

	1	**2·H₂O**	**3·37H₂O**	**4·17H₂O**	**5·28H₂O**	**6**
form	$C_{144}H_{252}Co_8N_{36}O_{60}S_{12}$	$C_{12}H_{23}CrN_6O$	$C_{96}H_{276}Cr_8N_{60}Ni_6O_{90}$	$C_{96}H_{258}Br_{12}Cr_8N_{48}Ni_6O_{45}$	$C_{120}H_{262}Cr_8N_{72}Ni_{12}O_{47}$	$C_{34}H_{70}Cl_2Cr_2N_{16}NiO_{10}$
form wt	4303.98	319.36	4480.03	4532.68	4586.54	1096.67
T, K	157	154	166	179	153	153
space group	$P2_1/c$	$P2_12_12_1$	$R\bar{3}$	$R\bar{3}$	$P2_1/n$	$Pca2_1$
Z	4	4	3	3	2	4
a, Å	26.7568(4)	8.3292(2)	25.1621(2)	19.4604(3)	18.4330(2)	28.9084(4)
b, Å	26.4830(3)	13.6144(4)			18.7475(6)	14.8794(2)
c, Å	27.0497(5)	13.6916(4)	29.2610(1)	41.7172(1)	31.6072(1)	11.4219(1)
β, deg	94.848(1)				102.009(2)	
V, Å³	19098.9(5)	1552.59(7)	16044.0(2)	13682.0(3)	10683.5(4)	4913.0(1)
d_{calc}, g/cm³	1.497	1.366	1.391	1.650	1.426	1.483
R_1 (wR_2),[b] %	5.08 (11.64)	2.81 (6.68)	10.09 (25.23)	6.47 (20.16)	11.76 (26.21)	3.58 (9.05)

[a] Obtained with graphite monochromated Mo Kα ($\lambda = 0.71073$ Å) radiation. [b] $R_1 = \sum||F_o| - |F_c||/\sum|F_o|$, w$R_2 = \{\sum[w(F_o^2 - F_c^2)^2]/\sum[w(F_o^2)^2]\}^{1/2}$.

[(Me₃tacn)Cr(CN)₃] (2). A solution of $[(Me_3tacn)Cr(CF_3SO_3)_3]$ (5.0 g, 7.5 mmol) in 50 mL of DMSO was heated to 120 °C. Solid KCN (12 g, 180 mmol) was added, and the mixture was stirred and heated at 120 °C under a dinitrogen atmosphere for 24 h. Upon cooling to room temperature, 300 mL of CH₂Cl₂ was added with vigorous stirring. The mixture was chilled in an ice bath, and a yellow precipitate was collected by filtration. Warm DMF (60 °C, 250 mL) was passed through the solid on a sintered glass frit to separate the product from excess KCN. The yellow filtrate was reduced to a volume of 10 mL by heating at 50 °C under reduced pressure. This solution was chilled in an ice bath, and stirred vigorously while 100 mL of Et₂O was added. The ensuing yellow precipitate was collected by filtration, washed with Et₂O, and recrystallized from a minimal amount (ca. 6 mL) of hot water. Bright yellow crystals were collected by filtration, and washed with acetone (3 × 10 mL) and Et₂O (3 × 10 mL) to afford 1.6 g (69%) of product. Absorption spectrum (H₂O): λ_{max} (ϵ_M) 339 (52), 425 (43) nm. IR (KBr): ν_{CN} 2133 cm⁻¹. Anal. Calcd for $C_{12}H_{21}CrN_6$: C, 47.83; H, 7.02; N, 27.89. Found: C, 47.30; H, 7.16; N, 27.59.

[(Me₃tacn)₈Cr₈Ni₆(CN)₂₄](NO₃)₁₂·17H₂O (3). A solution of compound **2** (40 mg, 0.13 mmol) and Ni(NO₃)₂·6H₂O (29 mg, 0.10 mmol) in 10 mL of water was stirred and heated at reflux for 16 h. The orange solution was then concentrated to a volume of 2 mL, cooled to room temperature, and further concentrated to 1 mL by evaporation upon standing in air. The resulting orange crystals were collected by filtration, rinsed with 2 mL of Et₂O, and dried in air. A second crop of crystals was collected upon further evaporation of the filtrate to ca. 0.5 mL to yield a total of 50 mg (78%) of product. Absorption spectrum (H₂O): λ_{max} (ϵ_M) 472 (689) nm. IR: ν_{CN} 2183 (sh), 2156, 2118 (sh) cm⁻¹. ES⁺-MS: *m/z* 813 ($[3 - 4NO_3 - 17H_2O]^{4+}$), 638 ($[3 - 5NO_3 - 17H_2O]^{5+}$), 521 ($[3 - 6NO_3 - 17H_2O]^{6+}$). Anal. Calcd for $C_{96}H_{202}Cr_8N_{60}Ni_6O_{53}$: C, 30.24; H, 5.34; Cr, 10.91; N, 22.04; Ni, 9.24. Found: C, 30.72; H, 5.49; Cr, 10.45; N, 21.60; Ni, 8.90. The water content of this compound was confirmed by thermogravimetric analysis. Orange block-shaped crystals of $[(Me_3tacn)_8Cr_8Ni_6(CN)_{24}](NO_3)_{12}\cdot54H_2O$ (**3**·37H₂O) suitable for X-ray analysis were obtained directly from the reaction product prior to drying.

[(Me₃tacn)₈Cr₈Ni₆(CN)₂₄]Br₁₂·28H₂O (4). This compound was prepared from NiBr₂·3H₂O (27 mg, 0.10 mmol) by a procedure analogous to that described for the preparation of **3**. The product was obtained as 48 mg (69%) of orange solid. Absorption spectrum (H₂O): λ_{max} (ϵ_M) 463 (837) nm. IR: ν_{CN} 2175 (sh), 2148, 2111 (sh) cm⁻¹. ES⁺-MS: *m/z* 1156 ($[4 - 3Br - 28H_2O]^{3+}$), 847 ($[4 - 4Br - 28H_2O]^{4+}$), 662 ($[4 - 5Br - 28H_2O]^{5+}$), 538 ($[4 - 6Br - 28H_2O]^{6+}$). Anal. Calcd for $C_{96}H_{224}Cr_8N_{48}Ni_6O_{28}$: C, 27.28; H, 5.34; N, 15.91. Found: C, 27.35; H, 5.66; N, 15.98. The water content of this compound was confirmed by thermogravimetric analysis. Orange block-shaped crystals of $[(Me_3tacn)_8Cr_8Ni_6(CN)_{24}]Br_{12}\cdot45H_2O$ (**4**·17H₂O) suitable for X-ray analysis were again obtained directly from the reaction product prior to drying.

[(Me₃tacn)₈Cr₈Ni₆(CN)₂₄][Ni(CN)₄]₆·19H₂O (5). Compound **3** (150 mg, 0.040 mmol) was added to 20 mL of water, and the mixture was stirred and heated at reflux to give an orange solution. A solution of Na₂[Ni(CN)₄] (74 mg, 0.35 mmol) in 5 mL of water was added, and the ensuing mixture was boiled down to a volume of 10 mL. The orange

precipitate was collected by centrifugation; was washed with water (3 × 2 mL), ethanol (3 × 2 mL), and Et₂O (3 × 2 mL); and was dried in air to yield 110 mg (70%) of product. IR (KBr): ν_{CN} 2163, 2136 cm⁻¹. Anal. Calcd for $C_{120}H_{206}Cr_8N_{72}Ni_{12}O_{19}$: C, 35.31; H, 5.09; N, 24.71. Found: C, 35.51; H, 5.24; N, 24.70. The water content of this compound was confirmed by thermogravimetric analysis. Yellow-orange hexagonal prism-shaped crystals of $[(Me_3tacn)_8Cr_8Ni_6(CN)_{24}]$-$[Ni(CN)_4]_6\cdot47H_2O$ (**5**·28H₂O) were grown by allowing an aqueous solution of the product to evaporate slowly.

[(Me₃tacn)₂(cyclam)NiCr₂(CN)₆](ClO₄)₂·2H₂O (6). A solution of Ni(cyclam)(ClO₄)₂ (0.11 g, 0.24 mmol) in 15 mL of water was slowly added to a stirred solution of compound **2** (0.14 g, 0.48 mmol) in 50 mL of water. The resulting yellow-orange solution was heated at reflux until its volume was reduced to 20 mL. Yellow rectangular plate-shaped crystals suitable for X-ray analysis formed on cooling to room temperature. The crystals were collected by filtration and dried in air to afford 0.19 g (71%) of product. IR (KBr): ν_{CN} 2158, 2131 cm⁻¹. Anal. Calcd for $C_{34}H_{70}Cl_2Cr_2N_{16}NiO_{10}$: C, 37.24; H, 6.43; N, 20.44. Found: C, 37.20; H, 6.65; N, 20.21.

X-ray Structure Determinations. Structures were determined for the six compounds listed in Table 1. Single crystals were coated with Paratone-N oil, attached to glass fibers, transferred to a Siemens SMART diffractometer, and cooled in a dinitrogen stream. Initial lattice parameters were obtained from a least-squares analysis of more than 30 centered reflections; these parameters were later refined against all data. None of the crystals showed significant decay during data collection. Data were integrated and corrected for Lorentz and polarization effects using SAINT and were corrected for absorption effects using SADABS.

Space group assignments were based on systematic absences, *E* statistics, and successful refinement of the structures. Structures were solved by direct methods with the aid of successive difference Fourier maps and were refined against all data using the SHELXTL 5.0 software package. Thermal parameters for all non-hydrogen atoms were refined anisotropically, except for the partially occupied sites associated with disordered atoms in the structures of **3**·37H₂O, **4**·17H₂O, and **5**·28H₂O. The positions of the hydrogen atoms in the structure of compound **6** were located and refined using isotropic thermal parameters. Hydrogen atoms associated with solvate water molecules and disordered methylene carbon atoms were not included in the structural refinements. All other hydrogen atoms were assigned to ideal positions and refined using a riding model with an isotropic thermal parameter 1.2 times that of the attached carbon or nitrogen atom (1.5 times for methyl hydrogens). The $[(tacn)_8Co_8(CN)_{12}]^{12+}$ clusters in the structure of compound **1** are disordered over two externally indistinguishable orientations (one is shown in Figure 1), in which only the positions of the cyanide C and N atoms are reversed; an occupancy factor of 0.5C + 0.5N was assigned to each of the cyanide atom sites. Additionally, the oxygen atoms of one of the tosylate anions in this structure are disordered over two positions. Large thermal parameters obtained for the methylene carbon atoms in structure of **3**·37H₂O are attributed to variations in the Me₃tacn ligand conformations; however, attempts to model the effect as a disorder between two conformations did not improve the structural

refinement. Nitrate anions and solvate water molecules are extensively disordered throughout this structure and could not be reliably differentiated. Methylene carbon atoms in the structures of **4**·17H₂O and **5**·28H₂O were modeled as being disordered over two equally occupied positions, corresponding to two distinct Me₃tacn ligand conformations. Two of the bromide anions and all of the solvate water molecules in the structure of **4**·17H₂O were modeled as being disordered over multiple positions. Five of the solvate water molecules in the structure of **5**·28H₂O and one oxygen atom of a perchlorate anion in the structure of **6** were treated similarly. The final agreement factors (Table 1) for the structures of **3**·37H₂O, **4**·17H₂O, and **5**·28H₂O are high owing to the extensive disorder present in the crystals and the accompanying poor data quality.

Magnetic Susceptibility Measurements. DC magnetic susceptibility data were collected using a Quantum Design MPMS2 SQUID magnetometer at temperatures ranging from 2 to 295 K. Data were corrected for diamagnetic contributions using Pascal's constants. Samples for magnetization measurements were suspended in a petroleum jelly mull to prevent torquing of crystallites at high magnetic fields. The data were fit to theoretical models using a relative error minimization routine (MAGFIT 3.1),[12] except in the case of compound **3**, for which magnetic data were simulated using CLUMAG.[13] Reported coupling constants are based on exchange Hamiltonians of the form $\hat{H} = -2J \, \hat{S}_i \cdot \hat{S}_j$.

Other Physical Measurements. Absorption spectra were measured with a Hewlett-Packard 8453 spectrophotometer. Infrared spectra were recorded on a Mattson Infinity System FTIR spectrometer or on a Nicolet Avatar 360 FTIR spectrometer equipped with an attenuated total reflectance accessory. Mass spectrometric measurements were performed in the positive ion mode on a VG Quattro (Micromass) spectrometer or on a Bruker Apex II 7 T actively shielded FTICR mass spectrometer, both of which were equipped with an analytical electrospray ion source instrument. Thermogravimetric analyses were carried out in a dinitrogen atmosphere using a TA Instruments TGA 2950.

Results and Discussion

Cubic Co₈(CN)₁₂. High quality crystals of [(tacn)₈Co₈(CN)₁₂]-(C₇H₇SO₃)₁₂·24H₂O (**1**) were grown by slow evaporation of an aqueous solution. The structure obtained by X-ray analysis of one of these crystals (Table 1) is much improved over that reported previously.[3] Two significant issues concerning the cubic [(tacn)₈Co₈(CN)₁₂]¹²⁺ cluster (see Figure 1) are confirmed: the mean Co···Co edge dimension is 4.94(1) Å, and no water is located inside the cluster cage. In contrast, extended frameworks of solid Prussian blue analogues tend to exhibit cubic cages with slightly longer edge dimensions (5.05−5.36 Å), each enclosing either a water molecule or an alkali metal cation.[5−7] However, although the solid phases are typically formed by rapid growth from an aqueous solution at room temperature, the molecular cluster is assembled in a boiling aqueous solution, such that any water trapped in its cavity upon formation has ample opportunity to escape into the surrounding solvent. Evidently, the available thermal energy is sufficient for the water to pass through one of the cube faces, which feature openings with a minimum width of 1.7 Å, based on van der Waals radii and the structure of **1**. Overall, this process appears to be favored not only by entropy, but also by enthalpy, in that the water molecule is better stabilized by hydrogen bonding in the bulk aqueous solvent than inside the cluster cavity. When the water exits the cluster it creates a vacuum within the cube cavity, presumably causing the cluster cage to contract by a slight kinking of its bridging cyanide ligands away from linearity (as reflected in the Co−C−N and Co−N−C angles, which lie in the range 173.8(4)−178.3(4)°). Note that the work of compression would primarily involve changes in the Co−C and Co−N

(12) Schmitt, E. A. Ph.D. Thesis, University of Illinois at Urbana-Champaign, 1995.

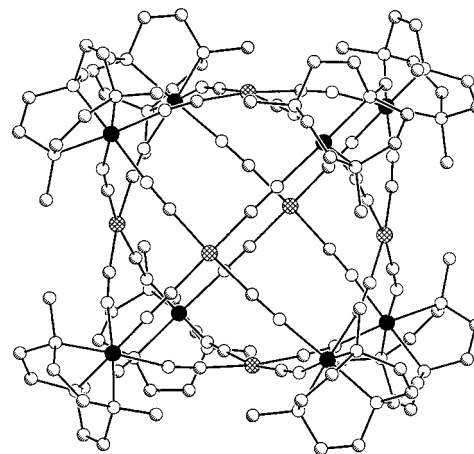(13) Gatteschi, D.; Pardi, L. *Gazz. Chim. Ital.* **1993**, *123*, 231.

Figure 2. Structure of the face-centered cubic cluster [(Me₃tacn)₈Cr₈-Ni₆(CN)₂₄]¹²⁺, as observed in **3**·37H₂O. Black, crosshatched, shaded, and white spheres represent Cr, Ni, C, and N atoms, respectively; H atoms are omitted for clarity. The cluster resides on a 3̄ symmetry site with the lower left back and upper right front Cr atoms positioned on the 3-fold rotation axis.

bond energies, limiting the extent of the contraction. A similar buckling effect has been observed in solid Prussian blue analogues, for which the unit cell dimension decreases upon dehydration due to kinking of the cyanide bridges.[14]

Face-Centered Cubic Cr₈Ni₆(CN)₂₄. As stated above, we are currently investigating modifications of reaction 1 in which only one reactant features a blocking tacn ligand, as a means of producing metal-cyanide clusters with high nuclearity. In view of the poor solubility of neutral [(tacn)M′(CN)₃] species, which is most likely a consequence of extensive hydrogen bonding in the solid state, Me₃tacn was instead employed as a capping ligand for this purpose. The precursor complex [(Me₃tacn)Cr-(CN)₃] was prepared by reacting [(Me₃tacn)Cr(CF₃SO₃)₃] with KCN in DMSO and is soluble in highly polar solvents such as acetonitrile, methanol, water, and DMF. In exploring its reactivity with selected paramagnetic transition metal ions, the following aqueous assembly reaction was quickly discovered.

$$8[(Me_3tacn)Cr(CN)_3] + 6[Ni(H_2O)_6]^{2+} \rightarrow$$
$$[(Me_3tacn)_8Cr_8Ni_6(CN)_{24}]^{12+} \quad (2)$$
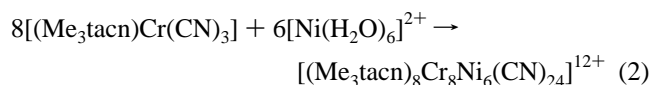
The orange cluster product is readily obtained in pure crystalline form with a variety of counteranions, including nitrate (**3**), perchlorate, chloride, and bromide (**4**), by utilizing the respective nickel salt. Interestingly, however, the use of NiI₂ as a reactant leads to formation of an incomplete Cr₈Ni₅ cluster.[15]

Single crystals of **3**·37H₂O and **4**·17H₂O, grown by slow evaporation of an aqueous solution, were subjected to X-ray analysis. The structure of the [(Me₃tacn)₈Cr₈Ni₆(CN)₂₄]¹²⁺ cluster (Figure 2) consists of a cubic arrangement of eight Me₃-tacn-terminated Cr atoms connected through bridging cyanide ligands to six square-planar Ni atoms situated just above the center of each cube face. Alternatively, the cluster can be viewed as an octahedron of Ni atoms with each face capped by a [(Me₃-tacn)Cr(NC)₃] unit, and, indeed, ignoring Me₃tacn ligand conformations, its point group symmetry is O_h. Selected mean interatomic distances and angles for the cluster are listed in Table

(14) (a) Herren, F.; Fischer, P.; Ludi, A.; Hälg, W. *Inorg. Chem.* **1980**, *19*, 956. (b) Beall, G. W.; Mullica, D. F.; Milligan, W. O. *Inorg. Chem.* **1980**, *19*, 2876.

(15) Sokol, J. J.; Shores, M. P.; Long, J. R. *Angew. Chem., Int. Ed.*, submitted for publication.

High-Nuclearity Metal-Cyanide Clusters

J. Am. Chem. Soc., Vol. 122, No. 40, 2000 9659

Table 2. Selected Mean Interatomic Distances (Å) and Angles (deg) for the $[(Me_3tacn)_8Cr_8Ni_6(CN)_{24}]^{12+}$ Clusters in $[(Me_3tacn)_8Cr_8Ni_6(CN)_{24}](NO_3)_{12}\cdot54H_2O$ (**3·37H₂O**), $[(Me_3tacn)_8Cr_8Ni_6(CN)_{24}]Br_{12}\cdot45H_2O$ (**4·17H₂O**), and $[(Me_3tacn)_8Cr_8Ni_6(CN)_{24}][Ni(CN)_4]_6\cdot47H_2O$ (**5·28H₂O**)[a]

	3·37H₂O	**4·17H₂O**	**5·28H₂O**
Cr$-$N$_{CN}$	2.016(9)	2.031(7)	2.03(1)
Ni$-$C	1.880(5)	1.873(9)	1.87(2)
C$-$N$_{CN}$	1.16(2)	1.145(6)	1.15(2)
Cr$-$N$_{tacn}$	2.053(9)	2.066(5)	2.07(2)
Cr⋯Ni	5.021(7)	5.019(2)	5.017(6)
Cr⋯Cr	6.98(9)	6.97(2)	7.00(1)
trans-Ni⋯Ni	8.802	8.844	8.65(3)
N$_{CN}$-Cr$-$N$_{CN}$	88.5(4)	88.0(3)	87.0(4)
Cr$-$N$_{CN}$-C	168(3)	169.1(5)	169(1)
C$-$Ni$-$C	89.7(7)	89.6(3)	89.8(5)
Ni$-$C$-$N	177(2)	177.6(3)	176(1)
N$_{CN}$-Cr$-$N$_{tacn}$	94.1(7)	94.4(2)	95.0(7)
N$_{tacn}$-Cr$-$N$_{tacn}$	83.2(4)	83.0(1)	83.0(7)

[a] N$_{CN}$ and N$_{tacn}$ indicate N atoms in cyanide and Me₃tacn ligands, respectively.

2. Note that there are no significant differences in its geometry between the nitrate and bromide salts. Overall, the metal-cyanide framework of the cluster forms a geodesic cage that defines a nearly spherical cavity with a volume of 284 Å³.[16] Surprisingly, neither crystal structure determination revealed any appreciable build-up of electron density inside the cavity that could be attributed to guest water molecules. This absence of water is supported by the positive ion electrospray mass spectra obtained for compounds **3** and **4**, which display peaks corresponding to the intact cluster, but none in which it is associated with water. We postulate that the volume and shape of the cavity preclude formation of a hydrogen-bonded structure that would stabilize a water cluster within its confines relative to the bulk solution. Passage through the rhombic $Cr_2Ni_2(CN)_4$ openings of the metal-cyanide cage is somewhat restricted by methyl groups from the Me₃tacn ligands, such that, based on van der Waals radii, the largest sphere that can freely move in and out is ca. 1.8 Å in diameter. As with the $[(tacn)_8Co_8(CN)_{12}]^{12+}$ cluster, it appears that the thermal energy available during synthesis is sufficient to force any entrapped water out through the cage openings. Although there is no source of coordination from inside the cluster, each of the square-planar Ni atoms exhibits a weak axial interaction with an exterior water molecule (Ni⋯O 2.455 Å) or bromide ion (Ni⋯Br 2.802 Å) in the structures of **3·37H₂O** and **4·17H₂O**, respectively.

Inherent to reaction 2 is a thermally activated linkage isomerization wherein the carbon end of cyanide shifts from ligating Cr^{III} in the $[(Me_3tacn)Cr(CN)_3]$ reactant to ligating Ni^{II} in the $[(Me_3tacn)_8Cr_8Ni_6(CN)_{24}]^{12+}$ product. The ensuing Cr$-$N$-$C$-$Ni connectivity was evident from a comparison of the C- and N-atom thermal parameters and overall residual factors in structural refinements performed using both possible cyanide ligand orientations. For example, upon reversing the cyanide ligand orientations in the refinement of the structure of **4·17H₂O**, the average isotropic thermal parameters for C and N change from 0.027 and 0.034 Å² to 0.020 and 0.047 Å², respectively, while R_1 increases from 6.47% to 6.92%. Additionally, the connectivity is consistent with the short Ni$-$C distances and with the Ni$-$C$-$N angles (175.4(9)$-$180(1)° in **3·37H₂O** and 177.2(6)$-$178.0(6)° in **4·17H₂O**) being closer to linearity than the Cr$-$N$-$C angles (164.6(7)$-$171.9(8)° in **3·37H₂O** and

(16) This volume is based on the van der Waals radii of the cluster atoms and was calculated using a previously described procedure: Shores, M. P.; Beauvais, L. G.; Long, J. R. *J. Am. Chem. Soc.* **1999**, *121*, 775.
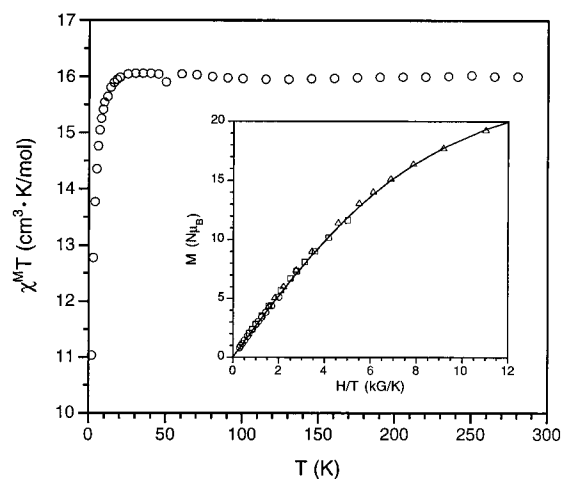

Figure 3. Magnetic behavior of compound **3**. Data represented by circles, squares, and triangles were measured in an applied field of 10, 25, and 50 kG, respectively. The solid line in the inset is the Brillouin function that corresponds to eight noninteracting $S = 3/2$ Cr^{III} ions.

168.6(6)$-$169.7(5)° in **4·17H₂O**) as a result of the more covalent interaction with the Ni centers. Simple thermodynamics dictates this cyanide orientation, with the softer carbon end preferring Ni^{II} over the harder Cr^{III} center, and similar instances of cyanide linkage isomerism have been documented in both molecular[17] and nonmolecular[6a,18] compounds. Of particular relevance here is the Prussian blue analogue $Fe_3[Cr(CN)_6]_2\cdot xH_2O$, in which a complete isomerization from Cr$^{III}-$C$-$N$-$Fe^{II} to Cr$^{III}-$N$-$C$-$Fe^{II} linkages is induced by heating the solid in air at 100 °C for several hours.[18a] Although theoretically predicted,[6a] an analogous isomerization involving Cr^{III} and Ni^{II} has not, to our knowledge, been demonstrated previously.

Reorientation of the cyanide ligands has a dramatic impact on the magnetic properties of the $[(Me_3tacn)_8Cr_8Ni_6(CN)_{24}]^{12+}$ cluster. The carbon end of cyanide presents a much stronger ligand field, prompting the Ni^{II} ions to adopt a square-planar coordination geometry (approximating that of $[Ni(CN)_4]^{2-}$) with a diamagnetic electron configuration. This eliminates the possibility of magnetic superexchange between the Cr and Ni centers, such that simple Curie-type behavior is expected for the cluster. Indeed, at temperatures above 30 K, the measured value of the $\chi^M T$ for compound **3** remains constant at approximately 16 cm³K/mol (see Figure 3), only slightly higher than the value of 15 cm³K/mol predicted for eight noninteracting $S = 3/2$ Cr^{III} ions with $g = 2.00$. However, when the temperature is lowered below 30 K, the $\chi^M T$ begins to decrease. As shown in the inset of Figure 3, the magnetization data for compound **3** closely follows the calculated Brillouin function, indicating that any zero-field splitting that is present is too small to account for the drop in the $\chi^M T$. Furthermore, intermolecular antiferromagnetic coupling is an unlikely source of this effect, because the intercluster separations between paramagnetic Cr^{III} ions in the structure of **3·37H₂O** are all greater than 10.8 Å. We, therefore, attribute the decrease to weak antiferromagnetic coupling between Cr^{III} centers within the cluster. A suitable superexchange pathway for the interaction makes use of the LUMO orbitals[19] of the $[Ni(CN)_4]^{2-}$-like units centering each cluster face:
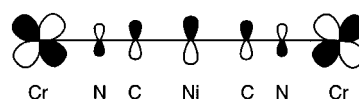
Note that an analogous orbital pathway couples the Cr^{III} ions disposed at *cis* positions on the $[Ni(CN)_4]^{2-}$ fragment. Simulations of the magnetic data in which each Cr^{III} ion was assumed to interact with six others (three located across a face diagonal and three across a cube edge) suggest that the magnitude of the long-range coupling is significantly less than 1 cm^{-1}. To our knowledge, this is the first observation of magnetic coupling between next-nearest metal ions in a cyano-bridged compound that is not a direct consequence of electron transfer (as in Prussian blue).[14a,20]

A number of approaches can be envisioned for achieving a high-spin ground state with the face-centered cubic cluster geometry introduced here. Perhaps the most straightforward of these involves carrying out the cluster assembly reaction at low temperature, so as to trap the kinetic product with Cr−C−N− Ni linkages prior to cyanide ligand rearrangement. The weaker ligand field enforced by the nitrogen end of cyanide[6a] should then maintain an $S = 1$ electron configuration for Ni^{II}, prompting ferromagnetic coupling with the surrounding Cr^{III} centers. Performing reaction 2 in methanol at −40 °C leads to the isolation of a green solid, which, upon warming to room temperature, gradually converts to an orange solid with spectral properties matching those of compound **3**. The magnetic behavior of this metastable green product is suggestive of the $S = 18$ ground state expected[9] for a putative $[(Me_3tacn)_8(H_2O)_{12}\text{-}Ni_6Cr_6(CN)_{24}]^{12+}$ cluster.[21] However, efforts to crystallize the compound at low temperature and confirm the face-centered cubic geometry are still in progress.[22] Note that of the numerous metal-oxo clusters examined for their magnetic properties, the highest ground-state spin yet reported is $S = 33/2$.[23,24] As alluded to earlier, a foreseeable advantage of metal-cyanide clusters is that once a new geometry is discovered, it should then be possible to construct analogues with a range of metal ions having similar coordination preferences. Thus, one means of stabilizing an $S = 18$ form of the face-centered cubic cluster would be to reduce the driving force for cyanide linkage isomerization by replacing its Cr^{III} ions with softer Mo^{III} or V^{II} ions. Indeed, the former substitution has already been accomplished, with isolation of an isomerized $[(Me_3tacn)_8Mo_8Ni_6(CN)_{24}]^{12+}$ cluster from high-temperature preparations.[25] Finally, replacing the Ni^{II} ions in the cluster with transition-metal ions that would remain paramagnetic upon isomerization (e.g., Mn^{II} or Co^{II}) could provide a route to magnetically coupled versions of the cluster. Precedence for such substitutions may be found in a series of isostructural phases $Cs_2[trans\text{-}M^{II}(H_2O)_2]_3[Re_6Se_8(CN)_6]_2\cdot xH_2O$ (M = Mn, Fe, Co, Ni, Cd), which feature a porous three-

(17) Lim, B. S.; Holm, R. H. *Inorg. Chem.* **1998**, *37*, 4898 and references therein.

(18) (a) Brown, D. B.; Shriver, D. F.; Schwartz, L. H. *Inorg. Chem.* **1968**, *7*, 77. (b) Brown, D. B.; Shriver, D. F. *Inorg. Chem.* **1969**, *8*, 37. (c) House, J. E., Jr.; Bailar, J. C., Jr. *Inorg. Chem.* **1969**, *8*, 672. (d) Reguera, E.; Bertrán, J. F.; Nuñez, L. *Polyhedron* **1994**, *13*, 1619.

(19) Demuynck, J.; Veillard, A. *Theor. Chim. Acta* **1973**, *28*, 241.

(20) Mayoh, B.; Day, P. *J. Chem. Soc., Dalton Trans.* **1976**, 1483.

(21) Here, the high-spin Ni^{II} centers are expected to exhibit an octahedral coordination environment composed of four nitrogen-bound cyanide ligands and two *trans* water ligands. The cluster cavity provides sufficient space for such coordination: assuming a Ni−O distance of 2.1 Å, the closest O···O contact between interior water molecules would be 3.3 Å.

(22) Sokol, J. J.; Shores, M. P.; Long, J. R., work in progress.

(23) Powell, A. K.; Heath, S. L.; Gatteschi, D.; Pardi, L.; Sessoli, R.; Spina, G.; Del Giallo, F.; Pieralli, F. *J. Am. Chem. Soc.* **1995**, *117*, 2491.

(24) Very recently, the potential for generating extremely high spin states in metal-cyanide clusters has been confirmed with species reported as exhibiting $S = 39/2$ and $S = 51/2$ ground states: (a) Zhong, Z. J.; Seino, H.; Mizobe, Y.; Hidai, M.; Fujishima, A.; Ohkoshi, S.; Hashimoto, K. *J. Am. Chem. Soc.* **2000**, *122*, 2952. (b) Larionova, J.; Gross, M.; Pilkington, M.; Andres, H.; Stoeckli-Evans, H.; Güdel, H. U.; Decurtins, S. *Angew. Chem., Int. Ed. Engl.* **2000**, *39*, 1605.

(25) Shores, M. P.; Sokol, J. J.; Long, J. R., manuscript in preparation.

Figure 4. Structure of the capped face-centered cubic cluster $[(Me_3\text{-}tacn)_8Cr_8Ni_6(CN)_{24}]\text{-}[Ni(CN)_4]_6$, as observed in **5**·28H$_2$O. Black, cross-hatched, shaded, and white spheres represent Cr, Ni, C, and N atoms, respectively; H atoms are omitted for clarity. The cluster resides on an inversion center in the crystal structure.

dimensional framework composed of analogous face-centered cubic cages, albeit with octahedral $[Re_6Se_8]^{2+}$ cluster cores in lieu of the Cr^{III} ions.[26]

Reaction with $[Ni(CN)_4]^{2-}$. While it seems unlikely that the Ni^{II} sites in $[(Me_3tacn)_8Cr_8Ni_6(CN)_{24}]^{12+}$ would have much affinity for an additional external ligand intended to alter their spin state, they do interact with $[Ni(CN)_4]^{2-}$ in a somewhat surprising fashion. Addition of $Na_2[Ni(CN)_4]$ to a concentrated aqueous solution of the cluster yields the orange solid $[(Me_3\text{-}tacn)_8Cr_8Ni_6(CN)_{24}][Ni(CN)_4]_6\cdot19H_2O$ (**5**). X-ray analysis of a crystal of **5**·28H$_2$O revealed an aggregate species in which a $[Ni(CN)_4]^{2-}$ unit caps each of the six Ni(CN)$_4$-centered faces of the cubic cluster, as shown in Figure 4. The capping interactions involve a mean Ni···Ni contact of 3.00(1) Å, with the cyanide ligands of the two tetracyanonickelate moieties arranged in a rigorously staggered geometry (the mean C−Ni···Ni−C torsion angle is 45(1)°). Similar interactions are present in the structure of Ba[Ni(CN)$_4$]·4H$_2$O, which contains one-dimensional stacks of staggered $[Ni(CN)_4]^{2-}$ units with a slightly longer Ni···Ni separation of 3.36 Å.[27] The shortest reported contact between *unsupported* square-planar Ni^{II} ions of which we are aware is 3.245 Å in nickel dimethylglyoxime.[28,29] These weak metal−metal bonding interactions are analogous to those frequently observed in structures containing square-planar Pt^{II} complexes,[30] and originate from admixing of empty p$_z$ orbitals with the filled d$_{z^2}$ orbitals of the Ni···Ni pairs. In the case of compound **5**, the bonding is most likely enhanced by two factors. First, the overall geometry of the cluster cage causes its $[Ni(CN)_4]^{2-}$ units to bow outward (as reflected in the mean C−Ni···Ni angle of 93(3)°), which permits a closer approach of the capping anion, while facilitating the mixing of

(26) Beauvais, L. G.; Shores, M. P.; Long, J. R. *Chem. Mater.* **1998**, *10*, 3783.

(27) Larsen, F. K.; Grønbaek Hazell, R.; Rasmussen, S. E. *Acta Chem. Scand.* **1969**, *23*, 61.

(28) Godycki, L. E.; Rundle, R. E. *Acta Crystallogr.* **1953**, *6*, 487.

(29) Much shorter Ni···Ni distances have been observed in clusters where the contact is enforced by bridging ligands. See: Lai, S.-Y.; Lin, T.-W.; Chen, Y.-H.; Wang, C.-C.; Lee, G.-H.; Yang, M.; Leung, M.; Peng, S.-M. *J. Am. Chem. Soc.* **1999**, *121*, 250 and references therein.

(30) Selected references: (a) Atoji, M.; Richardson, J. W.; Rundle, R. E. *J. Am. Chem. Soc.* **1957**, *79*, 3017. (b) Krogmann, K. *Angew. Chem., Int. Ed. Engl.* **1969**, *8*, 35. (c) Williams, J. M. *Adv. Inorg. Chem. Radiochem.* **1983**, *26*, 235. (d) Buss, C. E.; Anderson, C. E.; Pomije, M. K.; Lutz, C. M.; Britton, D.; Mann, K. R. *J. Am. Chem. Soc.* **1998**, *120*, 7783.
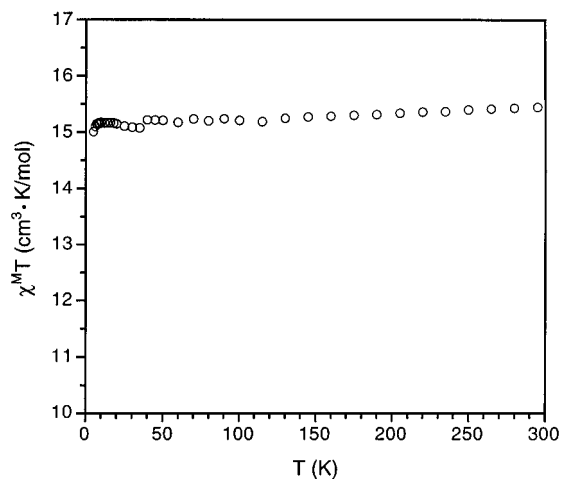
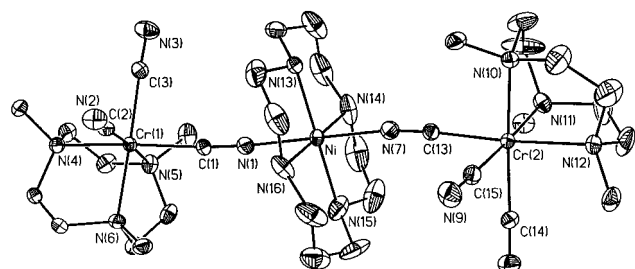**Figure 5.** Magnetic data for compound **5**, as measured in an applied field of 10 kG.

Figure 6. Structure of the linear $[(Me_3tacn)_2(cyclam)NiCr_2(CN)_6]^{2+}$ cluster in compound **6**, showing 40% probability ellipsoids and the core-atom labeling scheme; H atoms are omitted for clarity. Selected mean interatomic distances (Å) and angles (deg): Cr–C, 2.068(9); Ni–N_{CN}, 2.108(8); C–N_{CN}, 1.15(1); Cr–N, 2.107(3); Ni–N_{cyclam}, 2.072(3); C–Cr–C, 89(2); Cr–C–N, 176(2); Ni–N_{CN}–C, 170(1); N_{CN}–Ni–N_{CN}, 177.4(1); N_{CN}–Ni–N_{cyclam}, 90(1); N_{cyclam}–Ni–N_{cyclam}, 90(6); C–Cr–N, 94(2); N–Cr–N, 83.6(3).

the Ni p_z and d_{z^2} orbitals. Second, the inductive effect of the Cr^{III} ions in the cluster draws electron density away from the Ni^{II} centers, which increases their acidity in what can be viewed as an acid–base interaction between an empty Ni p_z orbital of the cluster and a filled Ni d_{z^2} orbital of the capping group. The infrared spectrum of a methanol solution of (sparingly soluble) compound **5** exhibits peaks with maxima at $\nu_{CN} = 2142$ and 2165 cm^{-1}, only slightly shifted from those observed in the solid state, and having no peak corresponding to free $[Ni(CN)_4]^{2-}$. Thus, it appears the capping interactions are robust enough that the $\{[(Me_3tacn)_8Cr_8Ni_6(CN)_{24}][Ni(CN)_4]_6\}$ aggregate remains intact in solution.

The magnetic behavior of compound **5** is wholly consistent with each tetracyanonickelate-capped cluster having eight magnetically isolated Cr^{III} ions. As shown in Figure 5, the measured value of the $\chi^M T$ remains approximately constant at just above the expected value of 15 cm^{3}K/mol over the entire temperature range from 4 to 295 K. Interestingly, the drop in the $\chi^M T$ observed at low temperature for compound **3** (see Figure 3) is not evident here, which indicates that the capping interactions disrupt the long-range antiferromagnetic coupling between the Cr^{III} centers in the cluster. This disruption is perhaps not unexpected, because the presumed superexchange pathway (see text drawing above) will be attenuated by the donation of electrons from the Ni d_{z^2} orbital of the capping anion into its Ni p_z orbital.

The resemblance of the face-capping interactions in compound **5** to the stacking interactions in the one-dimensional structure of $K_2[Pt(CN)_4]\cdot 3H_2O^{31}$ suggests another possible route
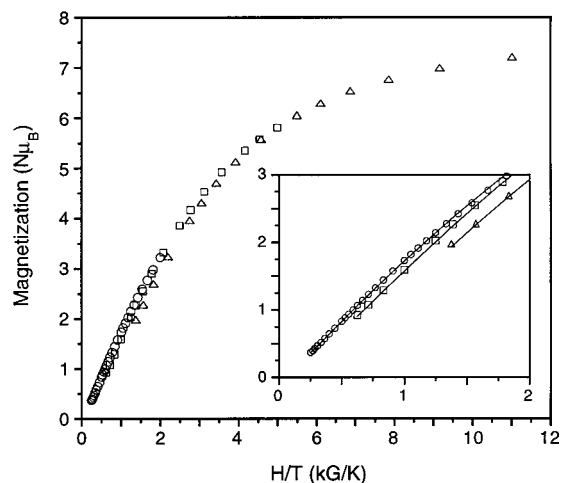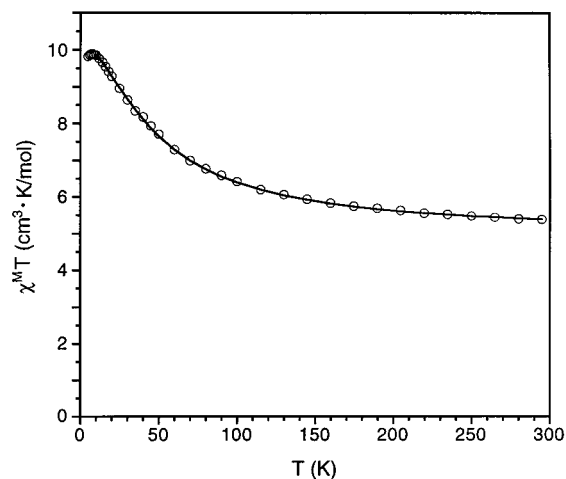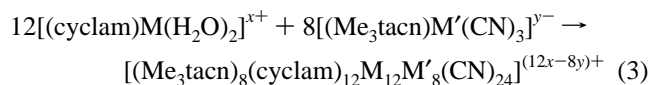

Figure 7. Magnetic behavior of compound **6**. Data represented by circles, squares, and triangles were measured in an applied field of 10, 25, and 55 kG, respectively. Solid lines represent calculated fits to the data; see text for details.

for enabling magnetic exchange coupling within the $[(Me_3tacn)_8Cr_8Ni_6(CN)_{24}]^{12+}$ cluster. Oxidized analogues of the tetracyanoplatinate compound can be prepared, in which partial depopulation of the Pt d_{z^2} orbitals enhances the metal–metal bonding and leads to electron delocalization along the mixed-valence chain.^{30bc} A similar oxidation of the Ni···Ni bonds in compound **5** could generate unpaired electron density on the Ni sites in the face-centered cubic cluster, invoking ferromagnetic exchange coupling with the surrounding Cr^{III} centers. Thus far, such an oxidized product has proved elusive; however, we note that substituting Pt for the 12 Ni centers in the compound should render a more accessible oxidation potential. Along this line of investigation, the reaction between $[(Me_3tacn)Cr(CN)_3]$ and $[PtCl_4]^{2-}$ in aqueous solution has been found to yield the required $[(Me_3tacn)_8Cr_8Pt_6(CN)_{24}]^{12+}$ precursor.^{22}

Linear NiCr$_2$(CN)$_6$. Employing 1,4,8,11-tetraazacyclotetradecane (cyclam) as a *trans*-directing ligand, we hope to use the following generic reaction to assemble still larger metal-cyanide clusters having spin states climbing as high as $S = 26$.

$$12[(cyclam)M(H_2O)_2]^{x+} + 8[(Me_3tacn)M'(CN)_3]^{y-} \rightarrow$$

$$[(Me_3tacn)_8(cyclam)_{12}M_{12}M'_8(CN)_{24}]^{(12x-8y)+} \quad (3)$$

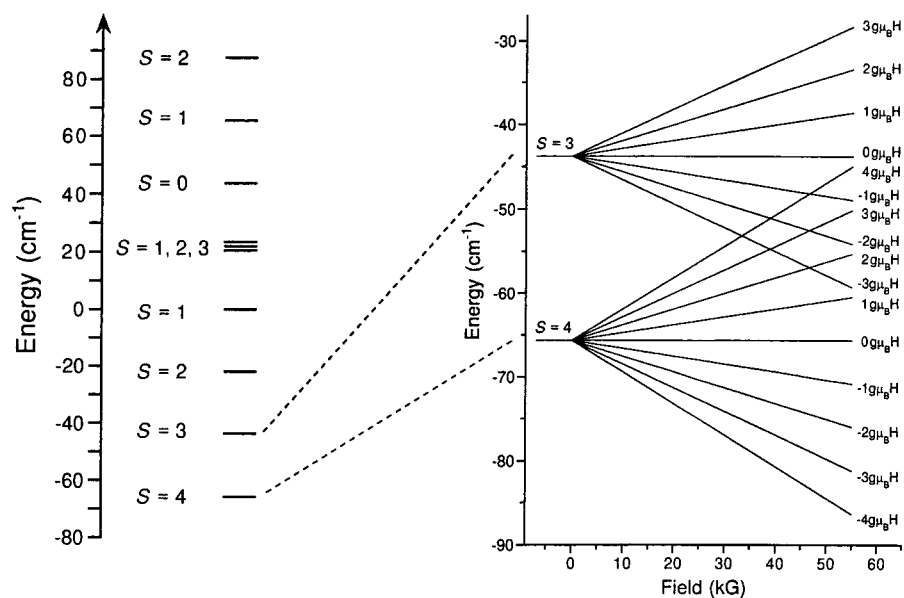The anticipated cluster geometry consists of an edge-bridged cube with 8 Me$_3$tacn-ligated M′ atoms defining the corners and

Figure 8. Spin ladder (left) and Zeeman splitting of the lowest energy states (right) for the linear $[(Me_3tacn)_2(cyclam)NiCr_2(CN)_6]^{2+}$ cluster, as calculated from the fit to the magnetic susceptibility data for compound **6** (Figure 7, upper).

a cyclam-ligated M atom centering each of the 12 M′−CN−M−NC−M′-linked edges. Precedence for this type of open metal-cyanide cage is established in the structure of $[Ni(en)_2]_3$-$[Fe(CN)_6](PF_6)_2$, where it comprises the fundamental building unit for an extended three-dimensional framework.[32] To date, efforts to crystallize an edge-bridged cubic cluster with a predicted $S = 24$ ground state from aqueous reactions between $[(cyclam)Ni(H_2O)_2](ClO_4)_2$ and $[(Me_3tacn)Cr(CN)_3]$ have been unsuccessful. However, in a 1:2 molar ratio, these reactants readily afford yellow crystals of $[(Me_3tacn)_2(cyclam)NiCr_2$-$(CN)_6]$-$(ClO_4)_2$·$2H_2O$ (**6**), featuring a linear cluster that represents a single edge fragment of the cube (see Figure 6).

A detailed examination of the magnetic properties of compound **6** was undertaken, because it provides a potentially useful model for interpreting the behavior of more complex clusters featuring $Cr^{III}−CN−Ni^{II}$ linkages, including the aforementioned metastable green product. As shown at the top of Figure 7, the susceptibility data exhibits a monotonic rise in the $\chi^M T$ with decreasing temperature, consistent with the predicted ferromagnetic coupling between octahedral Cr^{III} ($S = 3/2$) and Ni^{II} ($S = 1$) centers.[9] At low temperature, the $\chi^M T$ closely approaches the theoretical value of 10.0 cm³K/mol that is expected for the ensuing $S = 4$ ground state, but, at temperatures up to 295 K, the uncoupled limit of 4.75 cm³K/mol is not yet attained. Interestingly, as plotted at the bottom of Figure 7, the magnetization data for compound **6** shows an unusual trend in which the higher field curves drop beneath the lower field curves as the temperature of the sample increases (i.e., in following a curve from right to left). The origin of this effect is apparent from an accurate assessment of the energy states of the $[(Me_3tacn)_2$-$(cyclam)NiCr_2(CN)_6]^{2+}$ cluster, as obtained from a fit to the susceptibility data (Figure 7, upper) employing a single pairwise exchange parameter and an exchange Hamiltonian of the form

$$\hat{H} = -2J[\hat{S}_{Ni}·(\hat{S}_{Cr(1)} + \hat{S}_{Cr(2)})] \qquad (4)$$

The fit gives $g = 2.00$ and an exchange coupling constant of $J = 10.9$ cm⁻¹,[33] indicating a spacing of just 21.8 cm⁻¹ between nondegenerate energy states in the spin ladder of the molecule (Figure 8, left). Assuming a linear dependence on the applied magnetic field, the Zeeman splitting of the M_S levels for the

two lowest energy states is depicted at the right in Figure 8. Note that their proximity results in a crossing of the levels at higher field strengths. Consequently, at a high magnetic field, the Zeeman splitting leads to population of levels from the $S = 3$ state as the temperature of the sample increases, causing a decrease in the magnetization relative to the lower field data at the same H/T. In support of this hypothesis, the magnetization calculated simply by imposing a Boltzman distribution on the energy level scheme for the appropriate field strength closely matches the observed data (see inset in Figure 7). We expect the effect observed here to be significantly amplified in magnetization data for larger chromium(III)−nickel(II)−cyanide clusters with a higher spin ground state; indeed, such has been the observation for the green solid obtained from reaction 2 at low temperature.[22]

Supporting Information Available: X-ray structural information for the compounds listed in Table 1, including tables of crystal and refinement data, atomic positional and thermal parameters, and interatomic distances and angles. An X-ray crystallographic file (CIF). This material is available free of charge via the Internet at http://pubs.acs.org.

(31) (a) Moreau-Colin, M. C. *Bull. Soc. R. Sci. Liege* **1965**, *34*, 778. (b) Washecheck, D. M.; Peterson, S. W.; Reis, A. H., Jr.; Williams, J. M. *Inorg. Chem.* **1976**, *15*, 74.

(32) Fukita, N.; Ohba, M.; Okawa, H.; Matsuda, K.; Iwamura, H. *Inorg. Chem.* **1998**, *37*, 842.

(33) This is slightly stronger than the coupling ($J = 8.4$ cm⁻¹) observed in a heptanuclear $Ni_6Cr(CN)_6$ cluster with analogous exchange pathways.[4a]